Mechanics of Advanced Composite Structures 9 (2022) 115 – 123

Semnan University

Mechanics of Advanced Composite Structures

journal homepage: https://MACS.journals.semnan.ac.ir

Thermal Variations of Thermo-Mechanical Loading Effects on Creep Stress and Strain Distribution in Multi-layered Composite Cylinder

K. Hosseinpour, A. R. Ghasemi *

Department of Solid Mechanics, University of Kashan, Kashan, Iran

KEYWORDS

Thermo-mechanical loading;
Thermal variation;
Multilayer composites;
Integral model;
Viscoelastic creep.

ABSTRACT

In this research, thermal variation and internal pressure effects on stresses and strains of the creep behavior of composite laminates are investigated. Schapery's viscoelastic approach as a nonlinear model is used by Prandtl-Reuss theory and Mendelson's approximation to explain the stress/strains creep treatment. History of the radial, circumferential, and axial creep stresses and strains of a laminated composite cylindrical shell made of the E-glass/Vinylester laminated composites are studied and examined. Different laminated sequences of lay-ups, linear variation of thermal loading, various composite materials accomplished with internal pressure loading are investigated. For this purpose, two laminated lay-ups as $[0_{10}/45_{10}/0_{10}/45_{10}]$ and $[0_{10}/90_{10}/0_{10}/90_{10}]$ are selected, and Schapery integral nonlinear viscoelastic model of creep stress and strain approach for the constitutive equation is used. It was believed that the circumferential creep strain and absolute values of axial and radial creep strains are increasing with time and Also, creep stresses/strains in the multilayer composite cross-ply $[0_{10}/90_{10}/0_{10}/90_{10}]$ is more than the $[0_{10}/45_{10}/0_{10}/45_{10}]$ laminated composite cylindrical shells.

1. Introduction

Laminated composite structures are widely used in structural engineering, vehicles, aerospace, building, and other industries. Researchers use linear and nonlinear viscoelastic approaches to describe the creep behavior of the polymer matrix composites (PMCs) under thermal and mechanical loading [1, 2]. However, PMCs generally exhibit nonlinear behavior and rate-dependent treatments in creep rupture. Lou and Schapery [3] presented a single integral model, which has been used to predict the time-dependent strains for PMCs [3]. Tuttle et al. [4] used the Schapery single integral model and classical laminate plate theory (CLPT) to study the creep behavior of graphite-epoxy composite materials. Their results demonstrated the long-term creep compliance for 90° and 10° off-axis unidirectional specimens is accurate to within 10 percent at 10^5 minutes. The creep strain behavior response using the Burgers approach investigated by Berardi et al. [5], and numerical results are presented.

Gudes et al. [6] used a numerical method based on the Schapery integral constitutive equation to study the creep behavior of T300/5280 laminates. Their observations demonstrated a good agreement between computed and experimental results. Fiber orientation is one of the essential parameters that affected the PMCs' mechanical characterization and creep responses behavior, studied by Papanicolaou et al. [7]. They studied the effect of fiber orientation on the nonlinearity parameters of the Schapery integral model. Their results showed that the increase in the values of nonlinear parameters occurs with increasing stress, while this behavior is stabilized by decreasing the fiber direction, except for nonlinear parameters. In another study, Muliana et al. [8] obtained linear and nonlinearity parameters of the Schapery integral model for glass/vinyl ester composites. They did their

* Corresponding author. Tel.: +98-31-55913430 ; Fax: +98-31-55913434
E-mail address: ghasemi@kashanu.ac.ir

DOI: 10.22075/macs.2022.24442.1358
Received 2021-09-04; Received in revised form 2022-01-22; Accepted 2022-02-21.

experiments for 0°, 45°, and 90° fiber angles. Sayyidmousavi et al. [9] studied the viscoelastic thermo-mechanical behavior of the high-temperature PMCs. Their results showed the importance of calculating the viscoelastic effect of the matrix material with increasing temperature.

Samareh-mousavi and Taheri-behrooz [10] proposed a new phenomenological residual resistance describing the residual strength data under arbitrary stress conditions and stable times for T300 / L20 unidirectional layers. Song et al. [11] constructed design stresses and design spaces for high-temperature carbon/polymer composites considering creep responses in polymers. They used the power-law model to model transient and steady-state creep to describe polyamide macroscopic creep responses.

Rathore et al. [12] studied the effect of temperature on the flexural and creep performance of glass/epoxy, carbon/epoxy, and glass/carbon/epoxy hybrid composites. Their results showed that with increasing temperature, both strength and stiffness of all-fiber composites continued to decrease to the highest test temperature (110 ° C). They also represent the synergistic effect of glass and carbon fibers on hybrid composites at high temperatures.

Multilayer composite cylinders are spread in environments with high temperatures and high internal pressure. Due to the importance of stress and strain distribution in the walls of the composite cylinders, researchers have performed many studies. Ghasemi and Hosseinpour [13-15] studied the creep stress and strain in laminated PMCs circular cylindrical shells. Thermal and mechanical loading on the filament-winding composite pipe was performed by Bakaiyan et al. [16]. Their results showed that the hoop to the axial stress ratio depends on the change in the fiber directions. Hocine et al. [17] presented an experimental and analytical study for metal pressure vessels reinforced with carbon-epoxy layers.

A numerical and analytical study of the functionally graded materials (FGMs) reinforced by multilayer composites was investigated by Ghasemi et al. [18] using the theory of infinitesimally small elasticity. Some researchers studied the thermal and mechanical nonlinear responses of T300/5208 composite circular cylindrical shells under the internal and external pressure accomplished with axial force [19-21]. The time-dependent radial, axial, hoop, and shear stress distributions in the thickness of the multi-layered T300/5208 cylinder presented by Guedes [19]. His results showed the importance of the viscoelastic effect on the evolution of the time-dependent internal stress field in thick-sheet cylinders. Poirette et al. [22] presented a new approach based on the time-dependent damage spectrum. They performed quasi-static, creep, and fatigue testing to characterize the composite structure's elastic, plastic, viscoelastic, and viscoplastic behavior. Furthermore, other researchers presented and examined the effect of seawater absorption on the long-term viscoelastic response of the glass/BMI laminated composites structures [23-24].

Due to the importance of stress and strain distribution in laminated composite cylindrical shells, the effect of laminated sequences, type of composite materials, linear thermal variations, and nonlinear viscoelastic behavior are presented in this research. For this goal, using the nonlinear viscoelastic approaches, internal pressure as mechanical loading accomplished with linear thermal temperature distribution in the thickness of the cylindrical are considered. Moreover, using different models and relations, the distribution of the radial, axial and circumferential creep stress and strain in the thickness of the cylindrical shell for long-term creep behavior are examined and discussed.

2. Thermal and Mechanical Loading Conditions

2.1. Geometry and Thermo-Mechanical Loading Conditions

A laminated multi-layered composite circular cylinder made of Vinyl-ester resin reinforced by E-glass fiber with an inner radius $r_i = 100$mm and outer radius $r_o = 120$mm is observed in Fig. 1 The length of the cylinder is high, and the plane strain condition can be used. The internal pressure of the cylinder is $P_i = 5$ MPa, and the axial symmetric thermomechanical loading is established.

The steady-state conditions, long lengths, and axial symmetric assumptions, the differential equation of heat conduction in the cylindrical coordinate system are as follows [15-16].

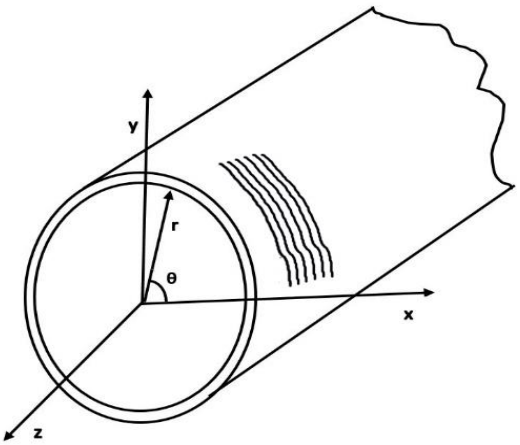

Fig. 1. Multi-layered composite cylindrical shell

$$\frac{\partial^2 T}{\partial r^2}+\frac{1}{r}\frac{\partial T}{\partial r}=0 \quad (1)$$

By solving Eq. (1), the temperature equation is obtained:

$$T = a\,ln(r)+b \quad (2)$$

where"a" and "b" are constant coefficients. Assuming that the outer surfaces have free convection to air at ambient temperature T_∞. And the inner surfaces have forced convection to the temperature of the hot fluid at T_f. The boundary conditions are as follows [16]:

$$\begin{aligned} -k\frac{\partial T}{\partial r} &= h_b(T-T_\infty) \qquad for \quad r=r_o \\ -k\frac{\partial T}{\partial r} &= h_a\big(T-T_f\big)* \qquad for \quad r=r_i \end{aligned} \quad (3)$$

Therefore

$$\begin{aligned} a &= \frac{(T_\infty - T_f)}{k\left(\frac{1}{r_o h_o}-\frac{1}{r_i h_i}\right)+ln\left(\frac{r_i}{r_o}\right)} \\ b &= \frac{k\left(\frac{T_f}{r_o h_o}-\frac{T_\infty}{r_i h_i}\right)+(T_f lnr_o - T_\infty lnr_i)}{k\left(\frac{1}{r_o h_o}-\frac{1}{r_i h_i}\right)+ln\left(\frac{r_i}{r_o}\right)} \end{aligned} \quad (4)$$

where k, h_a and h_b are thermal conduction (TC) of cylindrical shell, inner and outer average convection heat transfer coefficients. The following data are assumed in this research:

$T_f = 50^{\circ}C$ $\qquad$ $T_\infty = 25^{\circ}C$

$h_i = 50$ W/m°C $\qquad$ $h_o = 20$ W/m°C

2.2. Material Properties

The material properties of the E-glass/vinyl ester matrix are given in Table 1 based on the experimental results reported by Sawant et al. [25].

Table 1. Mechanical and thermal properties of E-glass/vinyl ester composites

E_x(MPa)	19268
E_y(MPa)	13210
G_{xy}(MPa)	4572
ϑ_{xy}	0.31
ϑ_{yz}	0.35
$\alpha_x(10^{-6}/°C)$	10
$\alpha_y(10^{-6}/°C)$	44
TC through the thickness (W/ m°k)	0.49

3. Schapery Non-linear Viscoelastic Model

A useful nonlinear viscoelastic model has been developed and demonstrated by Schapery [3-4, 15-16]. This method is fascinating because it allows us to describe a fundamental nonlinear phenomenon based on an integral relation. To model the creep behavior of the PMCs based on the nonlinear viscoelastic approach, in this research, Schapery's single integral model has been used.

At low-stress levels, the creep strain and stress can be related by strain compliance parameter, which is defined as follows:

$$D(t)=\frac{\varepsilon(t)}{\sigma_0} \quad (5)$$

where D(t) and ε(t) are creep compliance and creep strain, respectively. The Boltzmann's superposition principle to express time-dependent behavior for the low-stress levels can be presented as:

$$\varepsilon(t)=D_0\sigma_0+\int_0^t \Delta D\,(t-\tau)\frac{d\sigma}{d\tau}d\tau \quad (6)$$

The applied integral in this equation is known as the "hereditary integral" approach. The above equation shows that the strain at any given time depends on the entire stress history. Lou and Schapery [3] described the behavior of the nonlinear viscoelastic materials using expansion of the Eq. (6). The Schapery's single integral constitutive equation model under the uniaxial isothermal conditions can be expressed as [3]:

$$\varepsilon(t)=g_0D_0\sigma_0 + g_1\int_0^t \Delta D(\psi-\psi')\frac{d(g_2\sigma_0)}{d\tau}d\tau \quad (7)$$

where ΔD(ψ) is transient creep compliance and, ψ and ψ′ indicated the effects of time (reduced times) and can be defined as [3]:

$$\psi=\int_0^t \frac{dt'}{a_\sigma}, \quad \psi'=\psi(\tau)=\int_0^t \frac{dt'}{a_\sigma} \quad (8)$$

where g_0 g_1 g_2, and a_σ are stress-dependent nonlinear material parameters, which depend on the stress and temperature. Substituting the applied pressure (σ_0) into the Eq. (7), the creep strain is obtained as [3]:

$$\varepsilon(t)=g_0D_0\sigma_0+g_1g_2\Delta D(t/a_\sigma)\sigma_0 \quad (9)$$

Findley's power law is defined as follows:

$$\Delta D(t)=D_1t^n \quad (10)$$

Therefore, the creep strain relation can be written as follow:

$$\varepsilon(t)=g_0D_0\sigma_0+g_1g_2D_1(t/a_\sigma)^n\sigma_0 \quad (11)$$

where D_1 and n are independent of time and temperature and are obtained according to the linear viscoelastic behavior in the reference temperature. The nonlinear parameters of the GF/vinyl ester materials based on the Schapery constitutive equations have been mentioned as [25]:

$$\begin{aligned} g_0(\sigma_e) &= 1.004e^{\sigma_e 5.655\times10^{-4}} \\ g_1(\sigma_e) &= 3.55\times10^{-3}\sigma_e + 0.878 \\ g_2(\sigma_e) &= 9.83\times10^{-6}{\sigma_e}^2 \\ &\quad + 9.77\times10^{-3}\sigma_e + 0.636 \\ a_{\sigma_e} &= 1 \\ g_0(T) &= 1.872\times10^{-3}T + 0.866 \\ g_1(T) &= 1 \\ g_2(T) &= 1.259\times10^{-4}T^3 - 6.369\times10^{-3}T^2 \\ a_T &= 1 \end{aligned} \tag{12}$$

where σ_e is the effective stress that is octahedral stress and calculated by: $\sigma_e = \frac{1}{3}((\sigma_{rr}-\sigma_{\theta\theta})^2 + (\sigma_{rr}-\sigma_{zz})^2 + (\sigma_{zz}-\sigma_{\theta\theta})^2)^{\frac{1}{2}}$.

Furthermore, the linear parameters for GF/vinyl ester composites in Eq. (11) are shown in Table 2 [8].

Table 2. The linear viscoelastic parameters of the unidirectional E-glass/Vinyl-ester

Off-axis angle (θ)	0°	45°	90°
D_0*$10^{-5}(1/MPa)$	0.53	0.79	0.81
D_1*$10^{-5}(1/MPa)$	0.32	0.16	1.35
n	0.16	0.20	0.189

4. Theoretical Analysis

The stress and strain relations for the K[th] layer of the cylindrical shells can be presented as:

$$\begin{bmatrix}\sigma_{rr}\\ \sigma_{\theta}\\ \sigma_{zz}\\ \sigma_{\theta r}\\ \sigma_{zr}\\ \sigma_{z\theta}\end{bmatrix} = \begin{bmatrix}\bar{C}_{11} & \bar{C}_{12} & \bar{C}_{13} & 0 & 0 & \bar{C}_{16}\\ \bar{C}_{21} & \bar{C}_{22} & \bar{C}_{23} & 0 & 0 & \bar{C}_{26}\\ \bar{C}_{31} & \bar{C}_{32} & \bar{C}_{33} & 0 & 0 & \bar{C}_{36}\\ 0 & 0 & 0 & \bar{C}_{44} & \bar{C}_{45} & 0\\ 0 & 0 & 0 & \bar{C}_{45} & \bar{C}_{55} & 0\\ \bar{C}_{61} & \bar{C}_{62} & \bar{C}_{63} & 0 & 0 & \bar{C}_{66}\end{bmatrix}^{(k)} \times \left(\begin{bmatrix}\varepsilon_{rr}\\ \varepsilon_{\theta\theta}\\ \varepsilon_{zz}\\ \varepsilon_{\theta r}\\ \varepsilon_{zr}\\ \varepsilon_{z\theta}\end{bmatrix} - \begin{bmatrix}\varepsilon^c_{rr}\\ \varepsilon^c_{\theta\theta}\\ \varepsilon^c_{zz}\\ \varepsilon^c_{\theta r}\\ \varepsilon^c_{zr}\\ \varepsilon^c_{z\theta}\end{bmatrix} - \begin{bmatrix}\varepsilon^T_{rr}\\ \varepsilon^T_{\theta\theta}\\ \varepsilon^T_{zz}\\ \varepsilon^T_{\theta r}\\ \varepsilon^T_{zr}\\ \varepsilon^T_{z\theta}\end{bmatrix}\right) \tag{13}$$

where in the cylindrical system $(i;j = r,\theta,z)$, the ε^T_{ij}, ε^c_{ij} and ε_{ij} are the thermal strains, creep strains, and mechanical strains, respectively. Also, C^K_{ij} are the component of the stiffnesses matrix in the cylindrical coordinate for the k number of layers, which is obtained by multiple transfer matrix in the modulus matrix $\bar{C}^k_{ij}$ in the Cartesian coordinate systems [25].

The strain-displacement by the emphasis on $u_\theta = u_z = 0$ and radial displacement ($u_r(r)$) only depend on the radial direction, can be written as follows:

$$\begin{aligned} \varepsilon_{rr} &= \frac{\partial u_r}{\partial r} \\ \varepsilon_{\theta\theta} &= \frac{\partial u_\theta}{r\partial r} + \frac{u_r}{r} = \frac{u_r}{r} \\ \varepsilon_{zz} &= \frac{\partial u_z}{\partial z} = 0 \\ \varepsilon_{zr} &= \frac{\partial u_z}{\partial r} + \frac{\partial u_r}{\partial z} = 0 \\ \varepsilon_{\theta r} &= \frac{1}{r}\frac{\partial u_r}{\partial \theta} + r\frac{\partial}{\partial r}\left(\frac{u_\theta}{r}\right) = 0 \\ \varepsilon_{z\theta} &= \frac{\partial u_\theta}{\partial z} + \frac{1}{r}\frac{\partial u_z}{\partial \theta} = 0 \end{aligned} \tag{14}$$

Furthermore, the ε^T_{ij} can be obtained by:

$$\begin{aligned} \varepsilon^T_{rr} &= \alpha_r(T(r) - T_\infty) \\ \varepsilon^T_{\theta\theta} &= \alpha_\theta(T(r) - T_\infty) \\ \varepsilon^T_{zz} &= \alpha_z(T(r) - T_\infty) \\ \varepsilon^T_{\theta r} &= \alpha_{\theta r}(T(r) - T_\infty) \\ \varepsilon^T_{\theta z} &= \alpha_{\theta z}(T(r) - T_\infty) \\ \varepsilon^T_{rz} &= \alpha_{rz}(T(r) - T_\infty) \end{aligned} \tag{15}$$

According to the assumption considered, the equilibrium equations for the rotating cylinder are as follow:

$$\frac{\partial \sigma_{rr}}{\partial r} + \frac{\sigma_{rr} - \sigma_{\theta\theta}}{r} = 0 \tag{16}$$

$$\frac{\partial \sigma_{\theta r}}{\partial r} + \frac{2\sigma_{\theta r}}{r} = 0 \tag{17}$$

$$\frac{\partial \sigma_{zr}}{\partial r} + \frac{\sigma_{zr}}{r} = 0 \tag{18}$$

Substituting stress-strain relations from Eq. (14) into Eq. (13), and using Eq. (15), (2), and (16), the following differential equations are obtained:

$$\begin{aligned} r^2\frac{\partial^2 u_r^{(k)}}{\partial r^2} + r\frac{\partial u_r^{(k)}}{\partial r} - {\beta_1}^{(k)}{u_r}^{(k)} = \\ {\beta_2}^{(k)}\varepsilon_0 r + {\beta_3}^{(k)} r\Delta T + {\beta_4}^{(k)}\gamma_0 r^2 - {\beta_5}^{(k)} r^2\frac{\partial T}{\partial r} \end{aligned} \tag{19}$$

where

$$\beta_1{}^{(k)} = \frac{\bar{C}_{22}^{(k)}}{\bar{C}_{33}^{(k)}}$$

$$\beta_2{}^{(k)} = \frac{\bar{C}_{12}{}^{(k)} - \bar{C}_{13}{}^{(k)}}{\bar{C}_{33}{}^{(k)}}$$

$$\beta_3{}^{(k)} = \frac{(\bar{C}_{13}{}^{(k)} - \bar{C}_{12}^{(k)})\alpha_z^{(k)} + (\overline{C}_{23}^{(k)} - \bar{C}_{22}^{(k)})\alpha_\theta^{(k)} + \overline{(C}_{33}^{(k)} - \bar{C}_{23}^{(k)})\alpha_r^{(k)} + 2(\bar{C}_{36}^{(k)} - \bar{C}_{26}^{(k)})\alpha_{z\theta}^{(k)}}{\bar{C}_{33}^{k}} \quad (20)$$

$$\beta_4{}^{(k)} = \frac{\bar{C}_{26}{}^{(k)} - 2\bar{C}_{36}{}^{(k)}}{\bar{C}_{33}^{k}}$$

$$\beta_5{}^{(k)} = \frac{\bar{C}_{13}{}^{(k)}\alpha_z^{(k)} + \bar{C}_{23}{}^{(k)}\alpha_\theta^{(k)} + \bar{C}_{33}{}^{(k)}\alpha_r^{(k)} + 2\bar{C}_{36}{}^{(k)}\alpha_{z\theta}^{(k)}}{\bar{C}_{33}^{k}}$$

The solution for Eq. (19) can be obtained as:

$$u^{(k)} = X_1^{(k)} r^{D_1^{(k)}} + X_2^{(k)} r^{-D_1^{(k)}} + D_2^{(k)} r^4 + D_3^{(k)} r^3 + D_4^{(k)} r^3 ln(r) \quad (21)$$

where X_1^k and X_2^k are unknown constant integration coefficients, and other parameters are:

$$D_1{}^{(k)} = \sqrt{\beta_1{}^{(k)}}$$

$$D_2{}^{(k)} = \frac{(\bar{C}_{13}^{(k)} - \bar{C}_{12}^{(k)})\alpha_z^{(k)} + (\overline{C}_{23}^{(k)} - \bar{C}_{22}^{(k)})\alpha_\theta^{(k)} + \overline{(C}_{33}^{(k)} - \bar{C}_{23}^{(k)})\alpha_r^{(k)} + 2(\bar{C}_{36}^{(k)} - \bar{C}_{26}^{(k)})\alpha_{z\theta}^{(k)}}{\bar{C}_{33}{}^{k} - \bar{C}_{22}{}^{k}}$$

$$D_3{}^{(k)} = \frac{(\bar{C}_{12}^{(k)} - \bar{C}_{13}^{(k)})\varepsilon_0 + B(\bar{C}_{13}^{(k)}\alpha_z^{(k)} + \bar{C}_{23}^{(k)}\alpha_\theta^{(k)} + \bar{C}_{33}^{(k)}\alpha_r^{(k)} + 2\bar{C}_{36}^{(k)}\alpha_{z\theta}^{(k)} - 2\bar{C}_{33}^{(k)}D_2^{(k)})}{\bar{C}_{33}{}^{(k)} - \bar{C}_{22}{}^{(k)}} + D_2{}^{(k)}(A - T_\infty) \quad (22)$$

$$D_4{}^{(k)} = \frac{\overline{(C}_{26}{}^{(k)} - 2\bar{C}_{36}^{(k)})\gamma_0}{\overline{4C}_{33}{}^{(k)} - \bar{C}_{22}{}^{(k)}}$$

To calculate the unknown constant coefficients for each layer, we must use boundary conditions. For the N layer of the composite cylinder under axial symmetrical loading, assuming that the surface between the core and skin layers are minimal, the boundary conditions are expressed as [17]:

$$u_r^{(k)}(r_{(k)}) = u_r^{(k+1)}(r_{(k)})$$

$$\sigma_{rr}^{(k)}(r_{(k)}) = \sigma_{rr}^{(k+1)}(r_{(k)})$$

$$\sigma_{rr}^{(1)}(a) = -P_i$$

$$\sigma_{rr}^{(n)}(b) = 0 \quad (23)$$

$$2\pi \sum_1^n \int_{r_{k-1}}^{r_k} \sigma_z^{(k)}(r) r dr = 0$$

$$2\pi \sum_1^n \int_{r_{k-1}}^{r_k} \sigma_{z\theta}^{(k)}(r) r^2 dr = 0$$

In addition, the additional below boundary conditions could be allowed to obtain the other constants:

$$\sigma_{\theta r}^{(1)}(a) = \sigma_{zr}^{(1)}(a) = 0$$

$$\sigma_{\theta r}^{(n)}(b) = \sigma_{zr}^{(n)}(b) = 0$$

$$\sigma_{zr}^{(k)}(r_k) = \sigma_{zr}^{(k+1)}(r_k) \quad (24)$$

$$\sigma_{\theta r}^{(k)}(r_b) = \sigma_{\theta r}^{(k+1)}(r_k)$$

5. Time-Dependent Creep Analysis

To obtain the time-dependent creep analysis, the coefficients' creep stress and strain parameters must be considered. In this research, the Prandtl-Reuss relations are used. Also, the history of stress and strains vs. the time can be calculated using the expressed relations and Mendelson's approximation method for an extended period. In this approach, the thickness of the circular cylindrical shells is divided into the k increment. The authors explain the numerical procedure in the previous works [13-15].

6. Numerical Results and Discussions

Using the assumptions considered in the previous sections for material properties and thermo-mechanical loading, the creep stress and strain distribution in the cylindrical wall for different time steps were obtained. The history of radial, circumferential and axial creep stress and strain for two laminated sequences as $[0_{10}/90_{10}/0_{10}/90_{10}]$ and $[0_{10}/45_{10}/0_{10}/45_{10}]$, are plotted in Figs. 2 to 5. Values of creep strains that grow with times for the cross-ply laminates are shown in Fig. 2. History of the distribution radial, circumferential and axial creep strains ($\varepsilon_r^c, \varepsilon_\theta^c, \varepsilon_z^c$) in the dimensionless wall (r/b), the cross-ply laminates $[0_{10}/90_{10}/0_{10}/90_{10}]$ showed in Figs. 2-a, 2-b, and 2-c, respectively. The difference values of the creep strains between layers increased with increasing time.

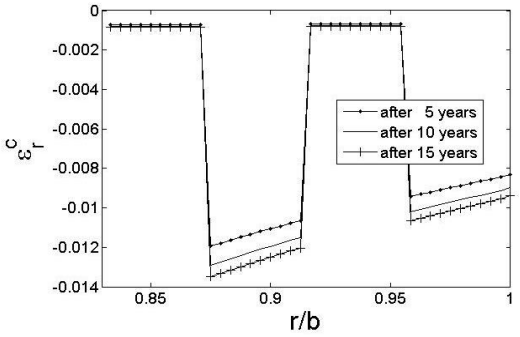

a

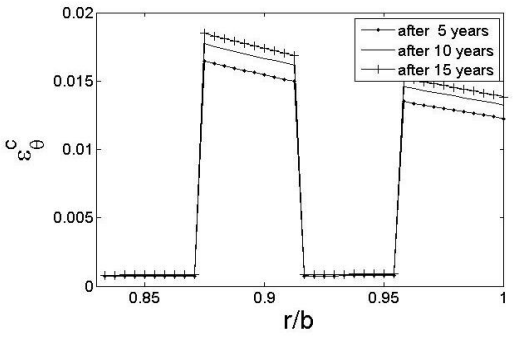

b

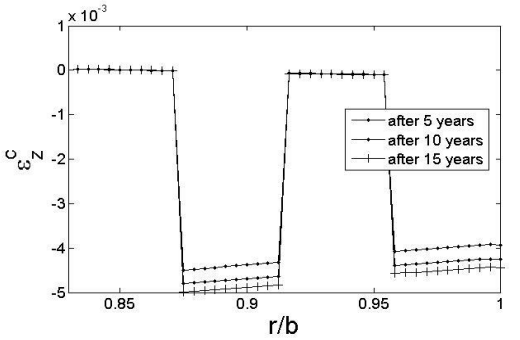

C

Fig. 2. Radial (a), circumferential (b), and axial creep strains for the composite cylinder with $[0_{10}/90_{10}/0_{10}/90_{10}]$ lay-ups

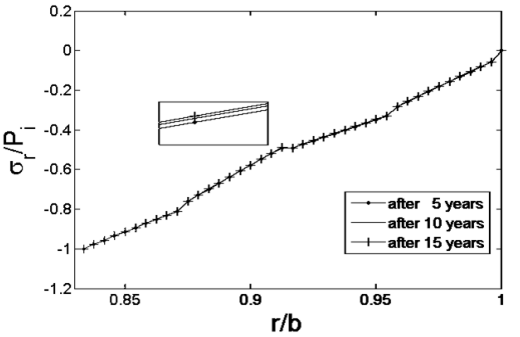

a

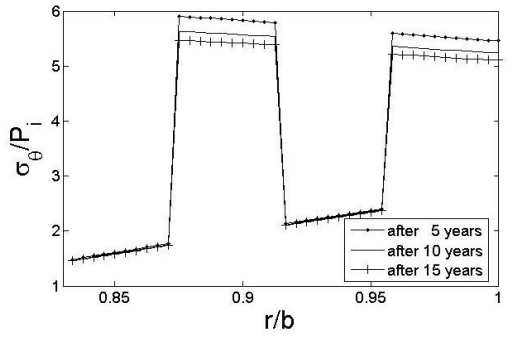

b

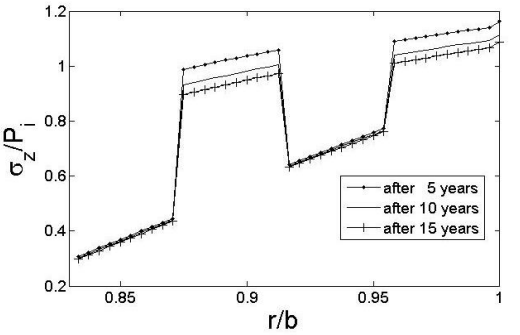

C

Fig. 3. Radial (a), circumferential (b), and axial creep stress for the composite cylinder with $[0_{10}/90_{10}/0_{10}/90_{10}]$ lay-up

Also, in each layer, by raising dimensionless radius, values of radial creep strains increased. Still, values of circumferential creep strains decreased that in layer with fiber angle 0° rate of change are lesser.

History of the dimensionless distribution radial, circumferential and axial stresses for the $[0_{10}/90_{10}/0_{10}/90_{10}]$ cross-ply laminates are plotted in Figs. 3-a, 3-b, and 3-c, respectively. Generally, the dimensionless effective stresses increase with time at a decreasing rate during the life of the cylindrical shell. Also, dimensionless values radial stress are continuous in the wall of the cylinder. On the other hand in dimensionless values of circumferential and axial stresses in the fiber angle 0° are very close together.

Fig. 4-a, 4-b and 4-c demonstrated the distribution of the axial, radial, and circumferential creep strains for laminated composite $[0_{10}/45_{10}/0_{10}/45_{10}]$ sequences. Fig. 4 Shows that values of creep strain increased with time, although in the fiber angle 0° the values of creep strains are increased is significantly lower than fiber angle 45°.

Also, with raising r/r_o in each layer, values of axial creep strains increased, but values of circumferential and radial creep strains decreased. Fig. 5 shows plotted variations of dimensionless radial, circumferential, and axial stresses. Changing procedure of the stresses are similar to $[0_{10}/90_{10}/0_{10}/90_{10}]$ laminated sequences. Also, dimensionless values of stresses in $[0_{10}/90_{10}/0_{10}/90_{10}]$ cross-ply sequences are more than dimensionless values of stresses in the $[0_{10}/45_{10}/0_{10}/45_{10}]$ laminated composite cylindrical shells.

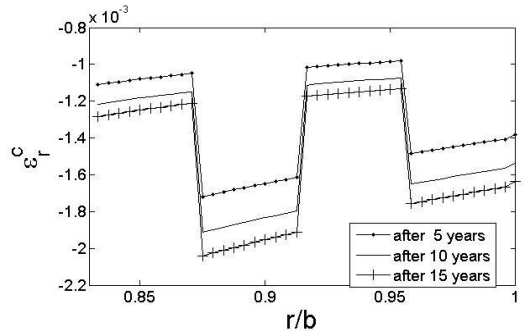

a

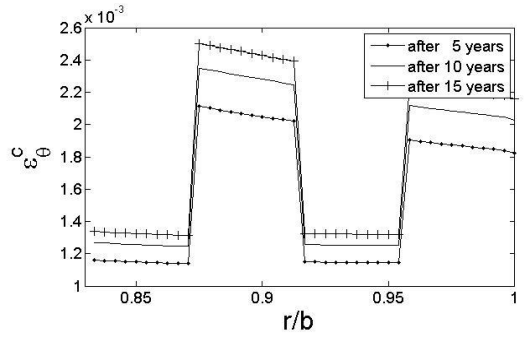

b

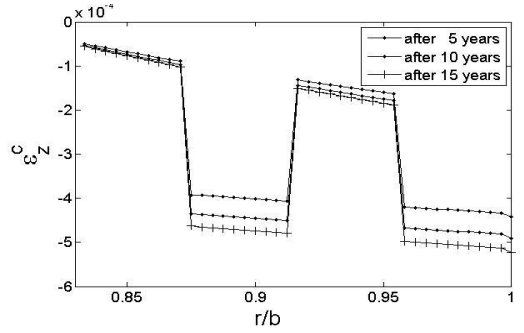

C

Fig. 4. Radial (a), circumferential (b), and axial creep strains for the composite cylinder with $[0_{10}/45_{10}/0_{10}/45_{10}]$ lay-ups

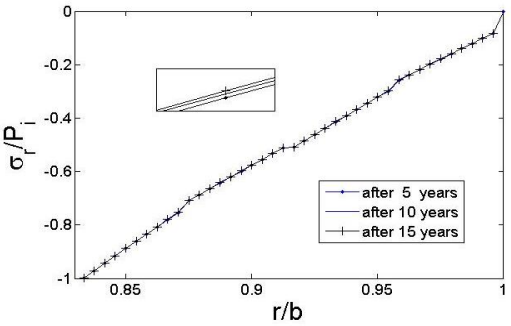

a

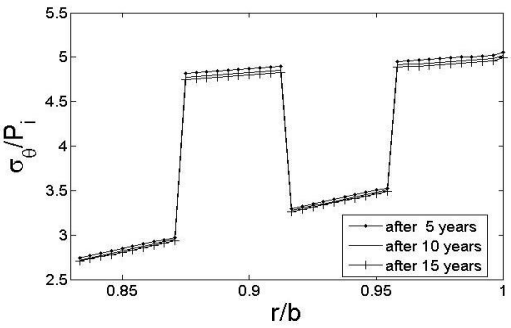

b

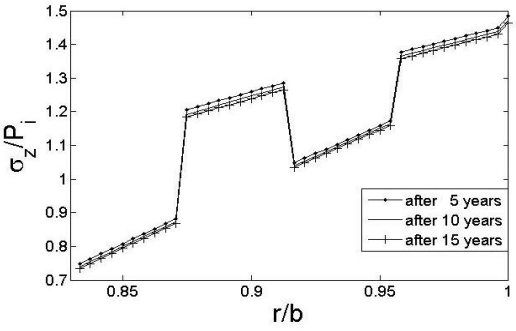

C

Fig. 5. Radial (a), circumferential (b), and axial creep stresses for the composite cylinder with $[0_{10}/45_{10}/0_{10}/45_{10}]$ lay-ups

Also, with raising r/r_o in each layer, values of axial creep strains increased, but values of circumferential and radial creep strains decreased. Fig. 5 shows plotted variations of dimensionless radial, circumferential, and axial stresses. Changing procedure of the stresses are similar to $[0_{10}/90_{10}/0_{10}/90_{10}]$ laminated sequences. Also, dimensionless values of stresses in $[0_{10}/90_{10}/0_{10}/90_{10}]$ cross-ply sequences are more than dimensionless values of stresses in the $[0_{10}/45_{10}/0_{10}/45_{10}]$ laminated composite cylindrical shells.

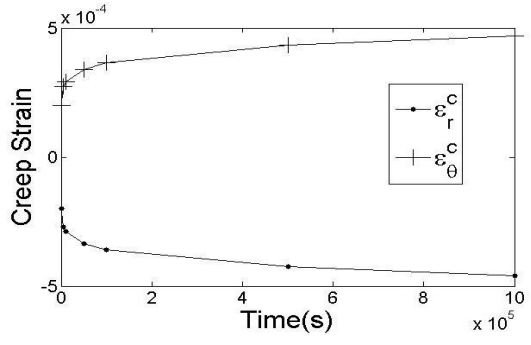

a

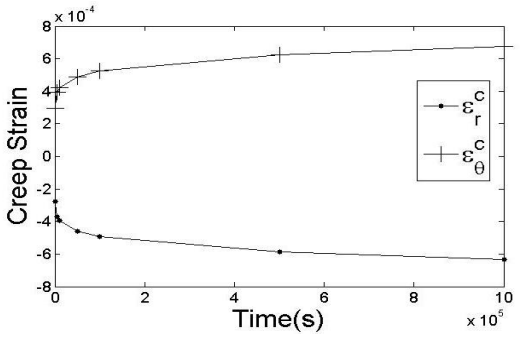

b

Fig. 6. Radial and circumferential creep strains variations versus the time for the composite cylinder with a) cross-ply $[0_{10}/90_{10}/0_{10}/90_{10}]$, and (b) $[0_{10}/45_{10}/0_{10}/45_{10}]$ lay-ups

Variation radial and circumferential creep strains in the cylinder's internal surface vs. time are demonstrated in Fig. 6-a and 6-b for two lay-ups. In Fig. 6 it is observed that with increasing the time, values of creep strains are increased in two lay-ups, but with increased time, the creep strain rate is slower. Figure 6 demonstrate at the beginning time, the rate of creep strain change in cross-ply $[0_{10}/90_{10}/0_{10}/90_{10}]$ lay-ups are more than that in $[0_{10}/45_{10}/0_{10}/45_{10}]$ lay-ups. Also, values of circumferential creep strain are higher than the values of the radial creep strains.

7. Validation of the Method

No research on the time-dependent creep of the pressure vessels or laminate composite structures have been founded, but to validate the results of this research, this method has been compared with the work of You et al. [26], which expressed the steady-state creep of functionally graded materials (FGM) under internal pressure.

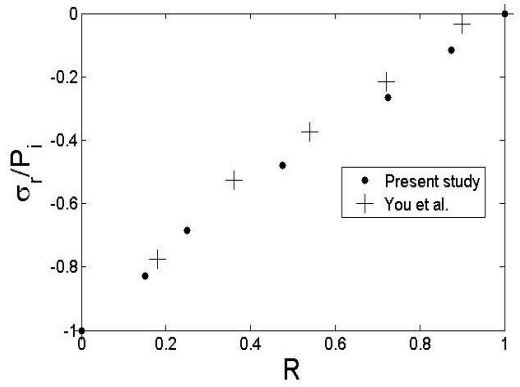

Fig. 7. Dimensionless radial stress variations in the wall of composite cylinder

Thus, using the analysis of You et al. [26] for the homogeneous material with the same geometry, our results for dimensionless compressive radial stress are shown in Fig. 7. In order to show the numerical results, the non-dimensional radial coordinate system is defined as:

$$R = \frac{r - r_a}{r_b - r_a} \tag{25}$$

Considering similar radial stresses calculated from both of these approaches, the validation of the present solution method can be examined in this respect.

8. Conclusions

The time-dependent creep treatment for laminated composite cylinders under combined thermo-mechanical loading and internal pressure were studied. Through the use of nonlinear viscoelastic model analysis and increment time approximation, the creep stress/strain was investigated.

The distribution of histories of radial, circumferential, ad axial creep stress and strain in the cylinder wall was obtained. It has been shown that dimensionless stresses and strain are increasing with time, and the rate of increase between 10 and 15 years is less than that of between 5 and 10 years. Despite values, the creep strains in $[0_{10}/45_{10}/0_{10}/45_{10}]$ lay-up are lower than $[0_{10}/90_{10}/0_{10}/90_{10}]$ cross-ply laminates. In $[0_{10}/45_{10}/0_{10}/45_{10}]$ lay-up and in fiber angle 45° changes of creep strains with time are very little. Also, in $[0_{10}/45_{10}/0_{10}/45_{10}]$ lay-up creep strains with less slope to reach steady-state than $[0_{10}/90_{10}/0_{10}/90_{10}]$ cross-ply laminated composite cylinder.

References

[1] Chen, D. L., Yang, P. F., and Lai, Y. S., 2012. A review of three-dimensional viscoelastic models with an application to viscoelasticity characterization using nanoindentation. *Microelectronics Reliability, 52(3)*, 541-558.

[2] Guedes, R. M., 2019. *Creep and fatigue in polymer matrix composites*. Woodhead Publishing.

[3] Lou, Y. C., and Schapery, R. A., 1971. Viscoelastic characterization of a nonlinear fiber-reinforced plastic. *Journal of Composite Materials, 5(2)*, 208-234.

[4] Tuttle, M. E., and Brinson, H. F., 1986. Prediction of the long-term creep compliance of general composite laminates. *Experimental Mechanics*, *26(1)*, 89-102.

[5] Berardi, V. P., Perrella, M., Armentani, E., and Cricrì, G., 2021. Experimental investigation and numerical modeling of creep response of glass fiber reinforced polymer composites. *Fatigue & Fracture of Engineering Materials & Structures*, *44(4)*, 1085-1095.

[6] Guedes, R. M., Morais, J. J., Marques, A. T., and Cardon, A. H., 2000. Prediction of the long-term behaviour of composite materials. *Computers & Structures*, *76(1)*, 183-194.

[7] Papanicolaou, G. C., Zaoutsos, S. P., and Kontou, E. A., 2004. Fiber orientation dependence of continuous carbon/epoxy composites nonlinear viscoelastic behavior. *Composites science and technology*, 64(16), 2535-2545.

[8] Muliana, A., Nair, A., Khan, K. A., and Wagner, S., 2006. Characterization of thermo-mechanical and long-term behaviors of multi-layered composite materials. *Composites Science and Technology*, 66(15), 2907-2924.

[9] Sayyidmousavi, A., Bougherara, H., Falahatgar, S. R., and Fawaz, Z., 2015. Thermomechanical viscoelastic response of a unidirectional graphite/polyimide composite at elevated temperatures using a

micromechanical approach. *Journal of Composite Materials*, *49(5)*, 519-534.

[10] Samareh-Mousavi, S. S., and Taheri-Behrooz, F., 2021. A new phenomenological creep residual strength model for the life prediction of the laminated composites. *Fatigue & Fracture of Engineering Materials & Structures*, *44(11)*, 3152-3168.

[11] Song, R., Muliana, A. H., and Palazotto, A., 2016. An empirical approach to evaluate creep responses in polymers and polymeric composites and determination of design stresses. *Composite Structures*, *148*, 207-223.

[12] Rathore, D. K., Prusty, R. K., Mohanty, S. C., Singh, B. P., and Ray, B. C., 2017. In-situ elevated temperature flexural and creep response of inter-ply glass/carbon hybrid FRP composites. *Mechanics of Materials*, *105*, 99-111.

[13] Ghasemi, A. R., and Hosseinpour, K., 2018. Thermo-magneto-mechanical long-term creep behavior of three-phase nano-composite cylinder. *Composites Science and Technology*, *167*, 71-78.

[14] Ghasemi, A. R., and Hosseinpour, K., 2018. The SWCNTs roles in stress/strain distribution of three-phase multi-layered nanocomposite cylinder under combined internal pressure and thermo-mechanical loading. *Journal of the Brazilian Society of Mechanical Sciences and Engineering*, *40(8)*, 1-14.

[15] Ghasemi, A. R., Hosseinpour, K., and Mohandes, M., 2018. Modeling creep behavior of carbon nanotube/fiber/polymer composite cylinders. *Proceedings of the Institution of Mechanical Engineers, Part N: Journal of Nanomaterials, Nanoengineering and Nanosystems*, *232(2-3)*, 49-58.

[16] Bakaiyan, H., Hosseini, H., and Ameri, E., 2009. Analysis of multi-layered filament-wound composite pipes under combined internal pressure and thermomechanical loading with thermal variations. *Composite Structures*, *88(4)*, 532-541.

[17] Hocine, A., Chapelle, D., Boubakar, M. L., Benamar, A., and Bezazi, A., 2009. Experimental and analytical investigation of the cylindrical part of a metallic vessel reinforced by filament winding while submitted to internal pressure. *International journal of pressure vessels and piping*, *86(10)*, 649-655.

[18] Ghasemi, A. R., Kazemian, A., and Moradi, M., 2014. Analytical and numerical investigation of FGM pressure vessel reinforced by laminated composite materials. *Journal of Solid Mechanics*, *6(1)*, 43-53.

[19] Guedes, R. M., 2010. Nonlinear viscoelastic analysis of thick-walled cylindrical composite pipes. *International Journal of Mechanical Sciences*, *52(8)*, 1064-1073.

[20] Hosseinpour, K., and Ghasemi, A. R., 2021. Agglomeration and aspect ratio effects on the long-term creep of carbon nanotubes/fiber/ polymer composite cylindrical shells. *Journal of Sandwich Structures & Materials*, *23(4)*, 1272-1291.

[21] Ghasemi, A. R., and Hosseinpour, K., 2018. Creep Strain and Stress Analysis in Laminated Composite Pressure Vessels. *Mechanics of Advanced Composite Structures*, *5(2)*, 141-147.

[22] Poirette, Y., Perreux, D., and Thiebaud, F., 2014. A contribution to time-dependent damage modeling of composite structures. *Applied Composite Materials*, *21(4)*, 677-688.

[23] Yian, Z., Zhiying, W., Keey, S. L., and Boay, C. G., 2015. Long-term viscoelastic response of E-glass/bismaleimide composite in seawater environment. *Applied Composite Materials*, *22(6)*, 693-709.

[24] Sawpan, M.A., 2021. Experimental Investigation of Long Term Seawater Durability and Shear Properties of Pultruded GFRP Composite. *Journal of Polymers and the Environment*, *29*(11), pp.3574-3586.

[25] Sawant, S., and Muliana, A., 2008. A thermo-mechanical viscoelastic analysis of orthotropic materials. *Composite Structures*, *83(1)*, 61-72.

[26] You, L.H., Ou, H. and Zheng, Z.Y., 2007. Creep deformations and stresses in thick-walled cylindrical vessels of functionally graded materials subjected to internal pressure. *Composite Structures*, *78*(2), pp.285-291.